

# PolypConnect: Image inpainting for generating realistic gastrointestinal tract images with polyps

Jan Andre Fagereng  
*Oslo Metropolitan University*  
Oslo, Norway  
andre\_fagereng@hotmail.com

Vajira Thambawita  
*SimulaMet*  
Oslo, Norway  
vajira@simula.no

Andrea M. Storås  
*SimulaMet*  
Oslo, Norway  
andrea@simula.no

Sravanthi Parasa  
*Swedish Medical Group*  
Seattle, WA, USA  
vaidhya209@gmail.com

Thomas de Lange  
*Sahlgrenska University Hospital, Gothenburg*  
Västra Götaland Region, Sweden  
thomas.de.lange@gu.se

Pål Halvorsen  
*SimulaMet*  
Oslo, Norway  
paalh@simula.no

Michael A. Riegler  
*SimulaMet*  
Oslo, Norway  
michael@simula.no

**Abstract**—Early identification of a polyp in the lower gastrointestinal (GI) tract can lead to prevention of life-threatening colorectal cancer. Developing computer-aided diagnosis (CAD) systems to detect polyps can improve detection accuracy and efficiency and save the time of the domain experts called endoscopists. Lack of annotated data is a common challenge when building CAD systems. Generating synthetic medical data is an active research area to overcome the problem of having relatively few true positive cases in the medical domain. To be able to efficiently train machine learning (ML) models, which are the core of CAD systems, a considerable amount of data should be used. In this respect, we propose the PolypConnect pipeline, which can convert non-polyp images into polyp images to increase the size of training datasets for training. We present the whole pipeline with quantitative and qualitative evaluations involving endoscopists. The polyp segmentation model trained using synthetic data, and real data shows a 5.1% improvement of mean intersection over union (mIOU), compared to the model trained only using real data. The codes of all the experiments are available on GitHub to reproduce the results.

**Index Terms**—polyp inpainting, synthetic polyps, generative models, synthetic medical data, fake polyp data

## I. INTRODUCTION

Utilizing the potential of data and deep learning in the medical sphere is a highly regarded and valuable task. Intelligent tools and computer-aided diagnosis (CAD) systems [1]–[3] can be developed in order to assist medical staff, in an effort to increase precision in diagnosis, support or guide in decision-making, or increase the general efficiency of medical processes. Even though there are clear potentials in utilizing artificial intelligence for such tasks, several challenges still exist to be researched.

One of the major issues in developing robust tools utilizing machine learning (ML) algorithms within the medical sphere is the lack of annotated data. Manual annotation of data by domain experts is a costly and time-consuming process, which is impractical in order to generate a substantially sized dataset for model consumption. Moreover, the manual data annotation process is subjective. As CAD systems potentially have an impact on the actions or decisions of doctors and medical

employees, it is crucial to obtain robust and reliable models. Models trained on small datasets might yield predictions with over-fit assumptions, not suitable for out-of-sample data and unfit for a production setting. The use of sensitive patient data can also give rise to privacy-related issues, which complicates the open sharing of data and code.

In this research, we aim to reduce or circumvent the issues above by producing machine-generated synthetic images with respective annotations in a selected medical case study, namely polyp segmentation [4]–[6]. More specifically, we apply image inpainting to generate gastrointestinal (GI) images containing polyps. Image inpainting can be described as a method that estimates pixel values to fill holes or missing areas in an image. By utilizing both unlabeled and labeled data, we train three image inpainting models and analyze the performance of generating polyps on clean-colon images. This is a suitable method since the mucosa surrounding the polyp is mostly completely normal. Finally, we introduce an effective polyp inpainting pipeline, called **PolypConnect**, to generate synthetic polyps in clean colon data based on the best findings of our experiments. This generation process is an effort to enlarge the size of the dataset and subsequently compare segmentation models trained on a mix of real and synthetic images to evaluate performance. The goal is to research if a generation of realistic images is viable for this kind of data and to what extent it has an impact on improving polyp segmentation models. Moreover, since the generated polyp images are not from real patients, this could be a way of circumventing regulations related to the privacy protection of sensitive medical data and sharing data more easily.

In this regard, we can list our main contributions as follows:

- We evaluate three different state-of-the-art image inpainting models for the GI tract and benchmark the best model in our polyp inpainting pipeline.
- We introduce PolypConnect, a novel polyp inpainting pipeline to convert non-polyp images (true-negative samples) to realistic polyp images (true-positive samples).

- We evaluate the quality of the pipeline quantitatively and qualitatively with the aid of medical experts.
- We evaluate the effectiveness of using synthetic polyp data for polyp segmentation models using the UNet architecture.

The code is available in <https://github.com/AndreFagereng/polyp-GAN> to reproduce the results and future studies, and this work is building upon the preliminary work published in an abstract by Thambawita et al. [7].

## II. RELATED WORK

Generating synthetic polyps is not a new research direction. However, producing realistic synthetic polyps with the corresponding ground truth, which can be used to train other machine learning models, is challenging. Random synthetic GI-tract images can be generated from the pre-trained generative adversarial network (GAN) models studied in [8], [9]. However, generating synthetic polyps and corresponding ground truth is not possible with these models.

One study developed an inpainting method for endoscopy medical images which was also able to remove specular highlights of polyps [10]. Akbari et al. [11] removed reflections in colonoscopy video frames using a proposed inpainting method. A GAN has also been developed to do inpainting reflections in endoscopic images [12]. Recently, Daher et al. developed a temporal GAN for the same purpose [13]. However, none of these methods are designed to inpaint synthetic polyps in clean GI images.

The SinGAN-Seg pipeline was introduced by Thambawita et al. [14] to generate synthetic polyps with the corresponding segmentation masks. Because this model uses only a single real polyp as an input, the generated samples show very close distributions of pixels to the input image. Furthermore, this model was developed to generate completely new synthetic polyp images from scratch and was not tested for converting non-polyp images into polyp images. Also, distributions of synthetic polyp images generated from this kind of pure polyp generators are showing quite similar distribution to the training data used to train GANs of the pipelines.

A simple UNET-based synthetic polyp generator was introduced by Qadir et al. [15]. In this study, they have experimented with converting polyp images into non-polyp and non-polyp into polyp images. However, the generated polyp can be discriminated easily based on the presented results. Furthermore, using only the mask to generate polyps makes generated polyps unrealistic, and the structure of the polyp can not be adjusted. In this regard, we present the PolypConnect pipeline to generate realistic synthetic polyp on clean colon images.

## III. POLYPCONNECT PIPELINE

The complete pipeline of PolypConnect is depicted in Figure 1. The pipeline consists of four steps. In **Step 1**, we use a GAN architecture to generate synthetic realistic polyp masks. In this study, we have used ProGAN [16]. However, other GAN architectures such as StyleGAN [17] and FastGAN [18]

can be used for the synthetic mask generation. The generated synthetic masks are then randomly paired with GI-tract images to produce images with missing regions. The EdgeConnect model is then pre-trained, conditioned on the missing region images and extracted edge maps.

In **Step 2**, we fine-tune the pre-trained EdgeConnect model using polyp datasets with corresponding extracted edge images. The pre-trained weights of the EdgeConnect model were loaded from Step 1. In this process, the model is trained to inpainting the exact polyp regions using the manually annotated ground truth provided in the datasets.

**Step 3** prepares the input data in order to produce realistic polyp output from non-polyp colon images. As a simple method, we extract polyp masks and the corresponding edge from the polyp datasets used in Step 2. Alternatively, polyp edge and corresponding masks can be generated using another GAN model. Then, extracted polyp edge is merged into the edge image of a clean colon image.

In **Step 4**, the edge polyp image returned from Step 3, the corresponding mask, and the clean colon image are provided as input to the pre-trained EdgeConnect model of Step 2. The generated polyp image is the final output of this PolypConnect pipeline. A sample clean-colon image and the generated polyp image generated using it are depicted in Figure 1.

## IV. EXPERIMENTAL RESULTS

### A. Data

For the purpose of training the models for the generation of synthetic polyps, we used the HyperKvasir dataset [19]. It consists of 1,000 images with segmented polyp annotations and around 100,000 unlabeled GI-tract landmarks. In Step 1, we have used the unlabeled data to pre-train the models. The segmentation dataset was used from Step 2 to the final polyp segmentation experiments. For the validation procedure, 200 images were randomly sampled from the training data, and therefore the models were trained with the remaining 800 images. This initial split (80/20) of the dataset was kept throughout all of the experiments, including the segmentation performed at the end. All the data used in this study are anonymous and publicly available for research purposes.

### B. Experimental setup

We used two GPUs of Geforce GTX TITAN X of 8 GB for the preliminary experiments. When the experiments were ready to run for a total number of epochs, an NVIDIA DGX server having 16 v100 GPUs of 32 GB was used, and the Pytorch deep learning framework version 1.10.1 was used for all experiments.

The structural similarity index (SSIM) [20], peak signal-to-noise ratio (PSNR) [21] and Fréchet inception distance (FID) [22] were used for quantitative evaluation of the models on the validation data. These metrics are commonly used to evaluate inpainting methods. Ideally, the SSIM and PSNR should be as high as possible, while the FID should be close to 0. In addition, a user survey including medical doctors was

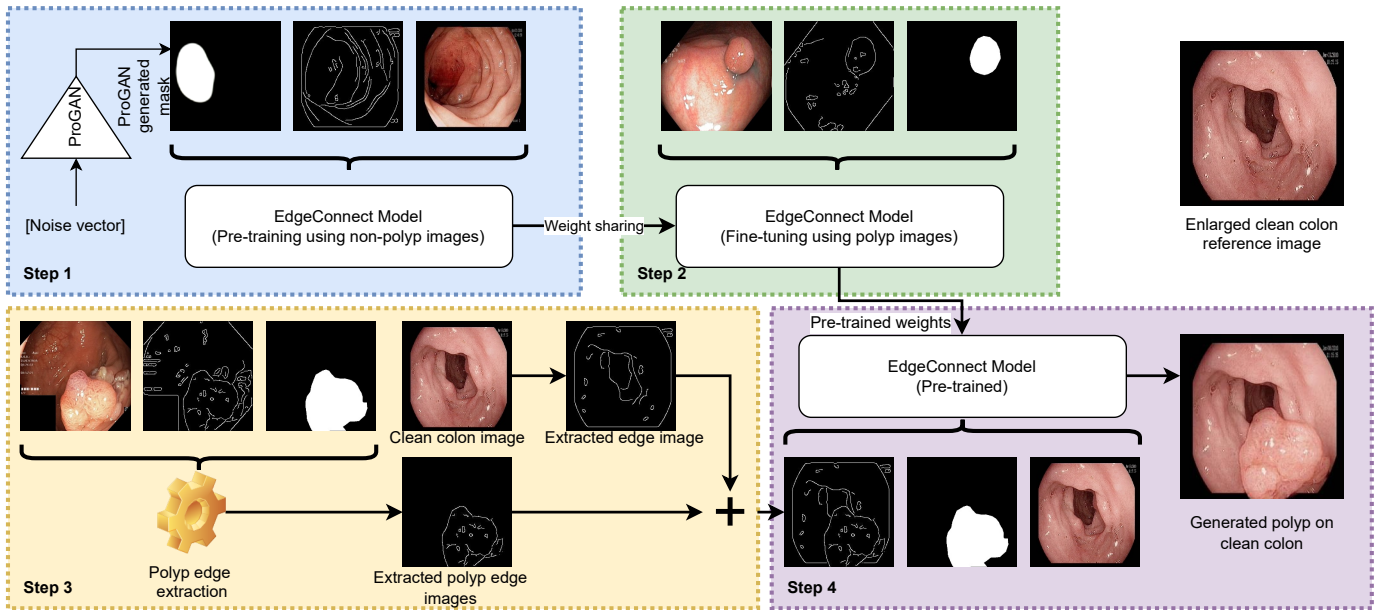


Fig. 1: Pipeline of PolypConnect. **Step 1** - Pre-training of EdgeConnect, **Step 2** - Fine-tuning of the EdgeConnect model, **Step 3** - Edge extractions for polyp masks (an alternative method is discussed in Section V), **Step 4** - Generating polyps on clean colon images.

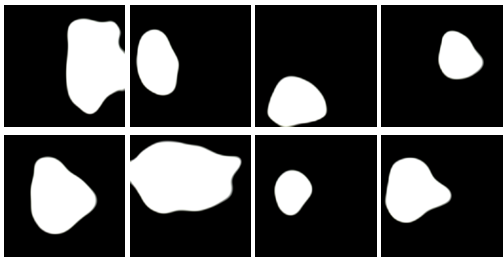


Fig. 2: Sample synthetic masks generated from ProGAN [16]

performed in order to evaluate the models qualitatively. Details about the survey are provided in subsection IV-G.

### C. Synthetic polyp masks

The total number of unique segmented polyp masks from KvasirSEG [23] is 1,000, which is insufficient for our preliminary experiments of general image inpainting. Thus, we used ProGAN [16] conditioned on random noise to produce new realistic polyp masks. Figure 2 visualizes some samples of the generated masks. Examining the generated masks, we observed a couple of undesirable shapes and sizes. The mask regions in these images were either taking up the entire region or were non-existent. In other words, the binary distribution of the masks was at each end of the extremes in these cases. Therefore, we decided to discard such images by only keeping generated images where the masked regions filled between 5% – 70% of the entire image.

### D. Polyp inpainting

We have selected three image inpainting models, namely GMCNN [24], AOTGAN [25] and EdgeConnect [26], to explore the capability of inpainting polyps on a given clean

TABLE I: Comparison of different image inpainting models. Selected best values from different checkpoints are presented here. The best two models' values are presented using **bold** text.

Model	SSIM	PSNR	FID
GMCNN [24]	0.4911	12.641	181.720
EdgeConnect [26]	<b>0.6100</b>	<b>17.980</b>	<b>74.070</b>
AOTGAN [25]	<b>0.9100</b>	<b>28.878</b>	<b>34.550</b>

colon image. These three models were chosen due to their popularity and novelty. We have performed a set of preliminary experiments, which are presented in Table I. Based on the preliminary results, we chose to proceed with EdgeConnect and AOTGAN.

### E. Selecting EdgeConnect over AOTGAN

The performance metrics for Edgeconnect and AOTGAN on the validation data after fine-tuning the models, are shown in Table II. In addition to qualitative evaluation, Figure 3 provides example data from the different steps of the PolypConnect pipeline using the EdgeConnect model and the AOTGAN model. Due to obvious visual differences in the generated polyps between the models, we selected the EdgeConnect model as the main polyp inpainting model of the PolypConnect pipeline for further evaluation and qualitative assessment by domain experts.

### F. Polyp segmentation models with synthetic polyps

At this stage of the experiments, the generated polyps from PolypConnect (using the EdgeConnect model as the main inpainting model) are prepared for the segmentation evaluation. In total, there are four datasets. Therefore, we

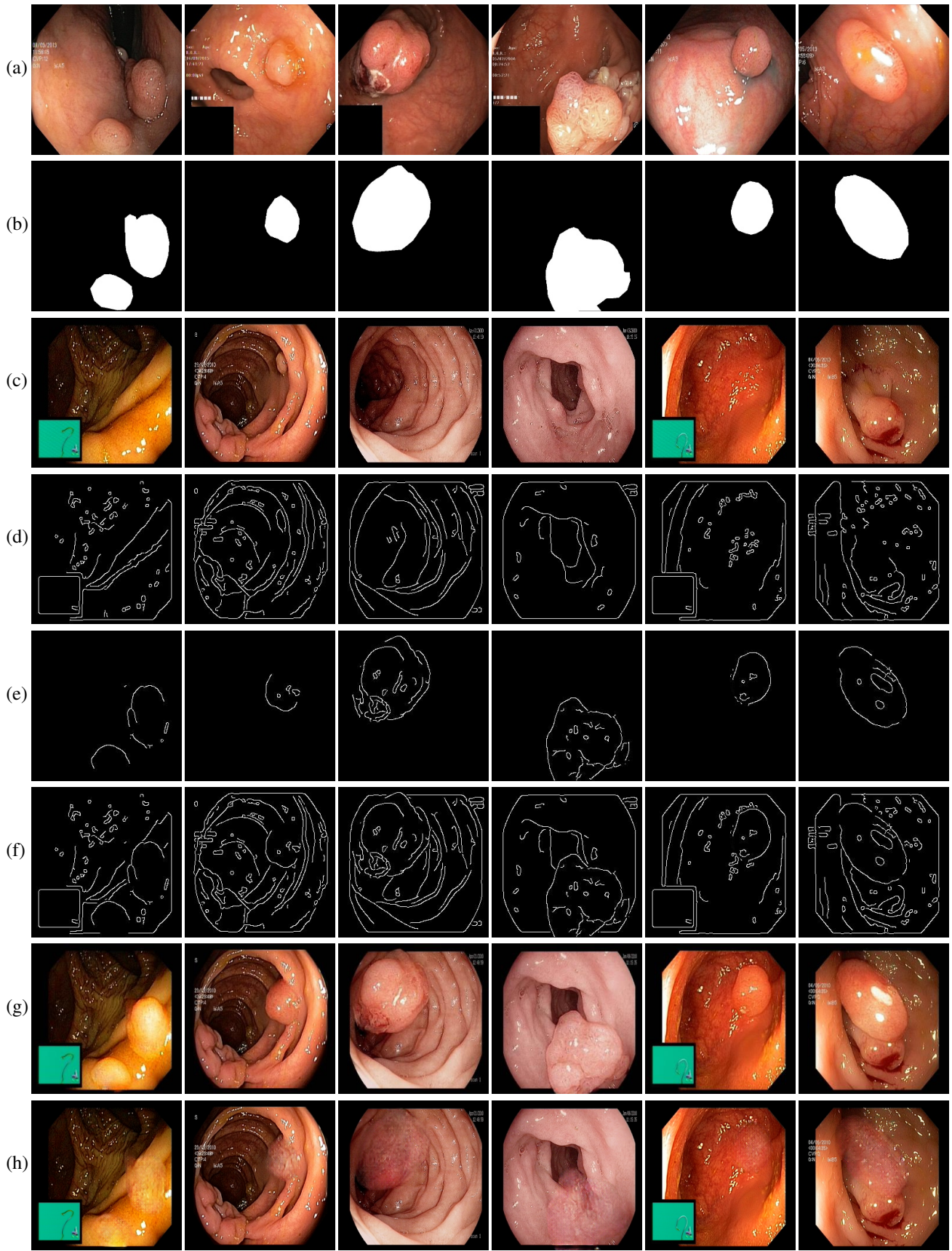


Fig. 3: Sample data used and generated in the different steps of PolypConnect pipeline. **(a)** - real polyp images, **(b)** - manually annotated polyp masks, **(c)** - randomly selected colon images used as input to the final step of PolypConnect, **(d)** - extracted edge images of row **c**. **(e)** - extracted edge images of polyp regions of row **a** using the masks of row **b**. **(f)** - combined edge images of row **d** and **e**. **(g)** - generated polyp on the images of row **c** using EdgeConnect. **(h)** - generated samples from AOTGAN.

TABLE II: Calculated metrics for fine-tuned Edgeconnect and AOTGAN on the validation set for different fine-tune iterations.

Model	EdgeConnect			AOTGAN		
	Iteration	SSIM	PSNR	FID	SSIM	PSNR
500	0.529	17.832	77.712	0.882	27.114	27.114
1000	0.527	17.859	77.007	0.890	28.176	42.102
2000	0.527	17.847	76.460	0.887	28.021	42.449
2500	0.526	17.836	76.956	0.889	27.969	42.484
3000	0.527	17.817	77.461	0.888	28.045	42.154
3500	0.527	17.817	77.515	0.888	28.038	42.559
4000	0.528	17.832	76.988	0.889	28.058	41.628
4500	0.526	17.796	76.851	0.889	28.084	41.599
5000	0.525	17.860	77.219	0.889	28.100	42.200
6000	0.527	17.835	76.310	0.882	28.0635	41.224

TABLE III: Evaluation of UNet segmentation model using real data and combined real and synthetic data. The best values are highlighted using **bold** text. Image IOU is calculated by aggregating intersection and union over whole dataset. Dataset IOU is also known as mIOU, and is the mean IOU.

Dataset	Image IOU	Dataset IOU	Dice Coef	Prec	Rec
Baseline	0.760	0.728	0.846	0.911	0.784
+800	<b>0.795</b>	<b>0.765</b>	<b>0.874</b>	<b>0.923</b>	0.817
+1600	0.791	0.758	0.869	0.912	<b>0.818</b>
+2400	<b>0.795</b>	0.759	0.873	0.919	0.814

train four U-Net [27] models for segmentation. The baseline dataset consists of only real polyp images. The remaining are datasets combining the real and generated polyp images. The first combined dataset consists of 800 real and 800 generated. The second and third are similar but with 1600 and 2400 generated polyp images. The models were evaluated on the same validation set of 200 real images. The obtained metrics show a clear improvement in all models trained on the additional synthetic data. Results can be found in Table III.

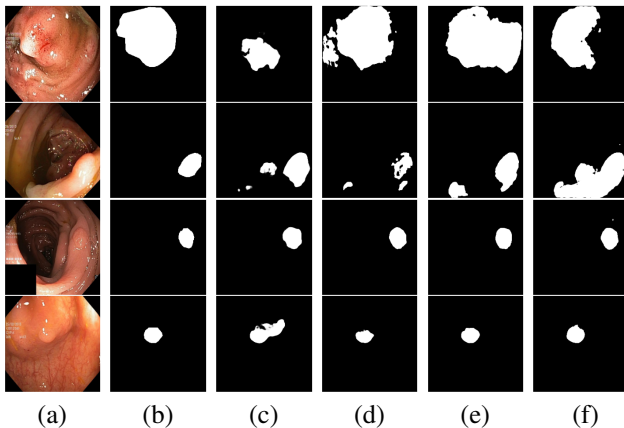


Fig. 4: Visual comparison of segmentation performance with UNet architecture when synthetic data is used. (a) Input Image. (b) Ground Truth. (c) Baseline (UNet) only with 800 real data (d) real data +800 (e) real data + 1600 (f) real data + 2400.

TABLE IV: Qualitative evaluation of synthetic polyps over real polyps using an questionnaire.

Reader	TP	FN	FP	TN	Accuracy	Recall	Precision
DOC	4	1	1	4	80%	80%	80%
DOC	3	2	3	2	50%	60%	50%
SAP	3	2	3	2	70%	80%	66%
GEC	4	1	3	2	60%	80%	57%
GEC	3	2	1	4	70%	60%	75%
GEC	3	2	3	2	50%	60%	50%
GEC	3	2	5	0	30%	60%	37.5%
Mean	-	-	-	-	<b>58.5%</b>	<b>68.5%</b>	<b>59.3%</b>

### G. Qualitative analysis by domain experts

Following the completion of the training and image inpainting of the generative models, a questionnaire was created to obtain subjective opinions on the generated images from domain experts. There were four participants in total from three fields of domain expert positions. Two of the participants are medical doctors (DOC), one is a gastroenterology consultant (GEC), and finally, an associate professor (SAP). The questionnaire included a total of ten polyp images and required the participants to rate images (fake or generated) on a confidence scale from 1 – 10, where a score of 1 means a real image, and a score of 10 means a generated image. To summarize the results, we converted these scores into binary (1 – 5 = real and 6 – 10 = generated). The summary of the collected results is tabulated in Table IV. In addition, the participants were asked to give the same confidence rating only based on the polyps themselves, and the background surrounding the polyps. The participants were not given any information regarding the experiment and had no knowledge about the study.

## V. DISCUSSION AND CONCLUSION

This study is focused on solving or reducing the data deficiency issues by efficiently generating realistic polyps in non-polyps images. This way, a dataset of finished segmented polyps can be generated in a short amount of time and vastly increase the data basis for polyp detection models. However, to be a useful solution, the generated results are required to be realistic and also improve the detection models experimentally. Our idea incorporated utilizing non-segmented and unlabeled data for pretraining the models on general GI-tract image inpainting prior to finetuning for polyp generation. We used ProGAN [16] to generate synthetic realistic polyp masks to be paired with random unlabeled images while training. However, we used the manually segmented polyp masks from KvasirSEG [23] to generate the synthetic polyps in non-polyp images. The polyp edges were extracted from the same images and used as the input for EdgeConnect. Synthetically generated pairs of polyp mask- and edge-images could be easily be created with ProGAN [16] or similar architectures, but this was not tested in this research. After conducting the experiments, we were able to generate realistic polyps in non-polyp images and also improve the detection rate of a polyp segmentation model by adding the synthetic data to the training data. The

improved metrics are presented in Table III. Precision and recall increased by 1.2% and 3.4%, respectively. Image IoU and dataset IoU increased from 0.76 to 0.795 (4.6%) and 0.728 to 0.765 (5.1%), respectively. The dice coefficient also showed improved results in the mixed datasets by 3.3%. All of the mixed datasets (utilizing the synthetic data) expressed clear improvements to the baseline. The model trained on the +800 dataset produced the overall best results. The +1600 and +2400 datasets yielded no clear improvement compared to the +800 dataset, and might therefore be an indication that additional synthetic images will not improve the segmentation model further. Moreover, the low accuracy of synthetic polyp detection by the domain experts presented in the results of the questionnaire implies that generated synthetic polyps are visually realistic as well.

## VI. FUTURE WORKS

The PolypConnect pipeline can be enhanced by adding more pre-extracted features, such as Histogram of Oriented Gradients and texture features, etc. Furthermore, different GAN architectures can be experimented with to generate synthetic polyp masks, synthetic edge images, and synthetic clean colon images as well. Investigating to control more fine features of generated data can add value to the pipeline.

## ACKNOWLEDGMENT

The research presented in this paper has benefited from the Experimental Infrastructure for Exploration of Exascale Computing (eX3), which is financially supported by the Research Council of Norway under contract 270053.

## REFERENCES

- [1] H. Lee and Y.-P. P. Chen, "Image based computer aided diagnosis system for cancer detection," *Expert Syst. Appl.*, vol. 42, no. 12, p. 5356–5365, jul 2015.
- [2] H.-P. Chan, L. M. Hadjiiski, and R. K. Samala, "Computer-aided diagnosis in the era of deep learning," *Medical Physics*, vol. 47, no. 5, pp. e218–e227, 2020. [Online]. Available: <https://aapm.onlinelibrary.wiley.com/doi/abs/10.1002/mp.13764>
- [3] J. Yanase and E. Triantaphyllou, "A systematic survey of computer-aided diagnosis in medicine: Past and present developments," *Expert Systems with Applications*, vol. 138, p. 112821, 2019. [Online]. Available: <https://www.sciencedirect.com/science/article/pii/S0957417419305238>
- [4] M. Yeung, E. Sala, C.-B. Schönlieb, and L. Rundo, "Focus u-net: A novel dual attention-gated cnn for polyp segmentation during colonoscopy," *Computers in Biology and Medicine*, vol. 137, p. 104815, 2021. [Online]. Available: <https://www.sciencedirect.com/science/article/pii/S00104825211006090>
- [5] Y. Guo, J. Bernal, and B. J. Matuszewski, "Polyp segmentation with fully convolutional deep neural networks—extended evaluation study," *Journal of Imaging*, vol. 6, no. 7, p. 69, 2020.
- [6] L. F. Sánchez-Peralta, L. Bote-Curiel, A. Picón, F. M. Sánchez-Margallo, and J. B. Pagador, "Deep learning to find colorectal polyps in colonoscopy: A systematic literature review," *Artificial intelligence in medicine*, vol. 108, p. 101923, 2020.
- [7] V. L. Thambawita, I. Strümke, S. Hicks, M. A. Riegler, P. Halvorsen, and S. Parasa, "Id: 3523524 data augmentation using generative adversarial networks for creating realistic artificial colon polyp images: Validation study by endoscopists," *Gastrointestinal Endoscopy*, vol. 93, no. 6, p. AB190, 2021.
- [8] V. Thambawita, S. A. Hicks, J. Isaksen, M. H. Stensen, T. B. Haugen, J. Kanters, S. Parasa, T. de Lange, H. D. Johansen, D. Johansen *et al.*, "Deepsynthbody: the beginning of the end for data deficiency in medicine," in *2021 International Conference on Applied Artificial Intelligence (ICAPAI)*. IEEE, 2021, pp. 1–8.
- [9] D. Yoon, H.-J. Kong, B. S. Kim, W. S. Cho, J. C. Lee, M. Cho, M. H. Lim, S. Y. Yang, S. H. Lim, J. Lee *et al.*, "Colonoscopic image synthesis with generative adversarial network for enhanced detection of sessile serrated lesions using convolutional neural network," *Scientific reports*, vol. 12, no. 1, pp. 1–12, 2022.
- [10] M. Arnold, A. Ghosh, S. Ameling, and G. Lacey, "Automatic segmentation and inpainting of specular highlights for endoscopic imaging," *EURASIP Journal on Image and Video Processing*, vol. 2010, pp. 1–12, 2010.
- [11] M. Akbari, M. Mohrekehsh, K. Najariani, N. Karimi, S. Samavi, and S. Soroushmehr, "Adaptive specular reflection detection and inpainting in colonoscopy video frames," in *2018 25th IEEE International Conference on Image Processing (ICIP)*, 2018, pp. 3134–3138.
- [12] I. Funke, S. Bodenstedt, C. Riediger, J. Weitz, and S. Speidel, "Generative adversarial networks for specular highlight removal in endoscopic images," in *Medical Imaging 2018: Image-Guided Procedures, Robotic Interventions, and Modeling*, B. Fei and R. J. W. III, Eds., vol. 10576. International Society for Optics and Photonics, 2018, pp. 8 – 16.
- [13] R. Daher, F. Vasconcelos, and D. Stoyanov, "A temporal learning approach to inpainting endoscopic specularities and its effect on image correspondence," 2022. [Online]. Available: <https://arxiv.org/abs/2203.17013>
- [14] V. Thambawita, P. Salehi, S. A. Sheshkal, S. A. Hicks, H. L. Hammer, S. Parasa, T. d. Lange, P. Halvorsen, and M. A. Riegler, "Singan-seg: Synthetic training data generation for medical image segmentation," *PLoS one*, vol. 17, no. 5, p. e0267976, 2022.
- [15] H. A. Qadir, I. Balasingham, and Y. Shin, "Simple u-net based synthetic polyp image generation: Polyp to negative and negative to polyp," *Biomedical Signal Processing and Control*, vol. 74, p. 103491, 2022.
- [16] T. Karras, T. Aila, S. Laine, and J. Lehtinen, "Progressive growing of gans for improved quality, stability, and variation," *arXiv preprint arXiv:1710.10196*, 2017.
- [17] T. Karras, S. Laine, and T. Aila, "A style-based generator architecture for generative adversarial networks," in *Proceedings of the IEEE/CVF conference on computer vision and pattern recognition*, 2019, pp. 4401–4410.
- [18] B. Liu, Y. Zhu, K. Song, and A. Elgammal, "Towards faster and stabilized gan training for high-fidelity few-shot image synthesis," in *International Conference on Learning Representations*, 2020.
- [19] H. Borgli, V. Thambawita, P. H. Smedsrud, S. Hicks, D. Jha, S. L. Eskeland, K. R. Randel, K. Pogorelov, M. Lux, D. T. D. Nguyen *et al.*, "Hyperkvasir, a comprehensive multi-class image and video dataset for gastrointestinal endoscopy," *Scientific data*, vol. 7, no. 1, pp. 1–14, 2020.
- [20] Z. Wang, A. Bovik, H. Sheikh, and E. Simoncelli, "Image quality assessment: from error visibility to structural similarity," *IEEE Transactions on Image Processing*, vol. 13, no. 4, pp. 600–612, 2004.
- [21] J. Korhonen and J. You, "Peak signal-to-noise ratio revisited: Is simple beautiful?" in *2012 Fourth International Workshop on Quality of Multimedia Experience*. IEEE, 2012, pp. 37–38.
- [22] M. Heusel, H. Ramsauer, T. Unterthiner, B. Nessler, and S. Hochreiter, "Gans trained by a two time-scale update rule converge to a local nash equilibrium," in *Advances in Neural Information Processing Systems*, I. Guyon, U. V. Luxburg, S. Bengio, H. Wallach, R. Fergus, S. Vishwanathan, and R. Garnett, Eds., vol. 30. Curran Associates, Inc., 2017.
- [23] D. Jha, P. H. Smedsrud, M. A. Riegler, P. Halvorsen, T. de Lange, D. Johansen, and H. D. Johansen, "Kvasir-seg: A segmented polyp dataset," in *International Conference on Multimedia Modeling*. Springer, 2020, pp. 451–462.
- [24] Y. Wang, X. Tao, X. Qi, X. Shen, and J. Jia, "Image inpainting via generative multi-column convolutional neural networks," *Advances in neural information processing systems*, vol. 31, 2018.
- [25] Y. Zeng, J. Fu, H. Chao, and B. Guo, "Aggregated contextual transformations for high-resolution image inpainting," *IEEE Transactions on Visualization and Computer Graphics*, 2022.
- [26] K. Nazeri, E. Ng, T. Joseph, F. Qureshi, and M. Ebrahimi, "Edgeconnect: Structure guided image inpainting using edge prediction," in *Proceedings of the IEEE/CVF International Conference on Computer Vision Workshops*, 2019, pp. 0–0.
- [27] O. Ronneberger, P. Fischer, and T. Brox, "U-net: Convolutional networks for biomedical image segmentation," in *International Conference on Medical image computing and computer-assisted intervention*. Springer, 2015, pp. 234–241.